Application of Graphene Oxide Membranes for Removal of Natural Organic Matter from Water

Y. You[1], X. H. Jin[1], X. Y. Wen[1], V. Sahajwalla[1], V. Chen[2], H. Bustamante[3], R. K. Joshi [1*]

[1]Centre for Sustainable Materials Research and Technology
School of Materials Science and Engineering, University of New South Wales, Sydney Australia
[2]UNESCO Centre for Membrane Science and Technology, School of Chemical Engineering, University of New South Wales, Sydney Australia
[3]Sydney Water, Parramatta, New South Wales 2125, Australia

Corresponding author's email: r.joshi@unsw.edu.au

Abstract

Changes in the complexity of natural organic matter (NOM) have impacted the performance of direct filtration plants of water industries, resulting in reduced treatment capacity, and can lead to increased disinfection by-products. Hence, the need to identify new materials in future can be converted into more effective technologies and processes. We report a laboratory scale innovative use of graphene oxide membranes to remove NOMs from water that had been treated and still contained 5 mg/L DOC. Our study shows that graphene oxide based membranes can reject ~100% of NOM while maintaining high water flux of 65 *L m^{-2} h^{-1} bar^{-1}* at atmospheric pressure. Our results indicate that it is possible to develop a graphene oxide-based water filtration technology.

1. Introduction

Natural organic matter (NOM) is ubiquitous in raw water that reaches water treatment plants[1]. Many water authorities have reported an increase in periods where coagulant and filter media are less effective for the removal of natural organic matter (NOM) and fine dispersed solids (turbidity)[1–7]. Changes in the complexity of natural organic matter (NOM) in Sydney's catchments has impacted the performance of direct filtration plants, resulting in reduced treatment capacity. The Nepean Water Filtration plant in Western Sydney has reduced its capacity by around 40% after some heavy rain events that increase NOMs in the raw water[8,9]. The length of time with reduced water produced is unpredictable and can last many weeks. Failure to successfully control the NOM issue could result in highly expensive to the treatment processes at Sydney's Water filtration plants in the next decade[10]. Hence the need to identify new alternatives that can potentially be converted into technologies to be retrofitted to existing water filtration plants.

Graphene oxide is a new material that is being widely researched to establish potential industrial applications[11–16]. Graphene oxide is a compound of carbon, oxygen, and hydrogen in a variable ratio that mainly depends on the synthesis procedure[17–19]. It can be prepared from graphite by introducing oxygenated functionalities using oxidizing agents[20,21]. These functionalities expand the layer separation between two stacked layers and make the material hydrophilic[22,23]. Although pristine graphene, a monoatomic layer of carbon atoms is completely impermeable to any gases or solutions, graphene oxide exhibits highly selective permeability to water molecules and has thus shown potential for applications in filtration material[17,24–28]. The advantage of graphene oxide-based membranes is that it can be prepared as laminates from stacks of graphene oxide monoflake using a very simple and cost-effective method[29]. In the laminated form, graphene oxide layers are stacked together (which is also known as graphene oxide paper[29]) with an interlayer distance of ~0.86 nm which is the path for mass transport of ions using it as a filtration membrane[17,30–32]. Based on the reported graphene oxide membrane characteristics, it appears that graphene oxide can offer 100% rejection for any species of a size equivalent to NOMs.

This paper describes laboratory scale studies to determine whether graphene oxide can be used to tackle the removal of NOMs in water. Hence, the objectives of this paper are two-fold, namely to establish whether graphene oxide (GO) membranes can reject NOM and to quantify water fluxes and whether the GO membranes get blocked during laboratory scale testing.

2. Experimental

2.1. Graphene oxide synthesis

Graphene oxide dispersions were prepared from graphite oxide which was synthesized using Hummer's method in which natural graphite was oxidized using appropriate quantity of sulfuric acid, potassium permanganate and sodium nitrate under controlled temperature[20]. The reaction mixture after treating with hydrogen peroxide was washed several times with de-ionized water to obtain graphite oxide paste. Later, the graphite oxide was exfoliated using ultra-sonication in water followed by centrifugation to obtain monolayer flakes of graphene oxide in water. Just to make it clear that the sonication exfoliates the individual layer of graphene oxide from the original graphite oxide in a similar way as graphene layers are exfoliated from natural graphite and subsequent centrifugation can separate out monolayer graphene oxides from multilayers. Schematic below (Fig. 1) shows the various steps of graphene oxide synthesis.

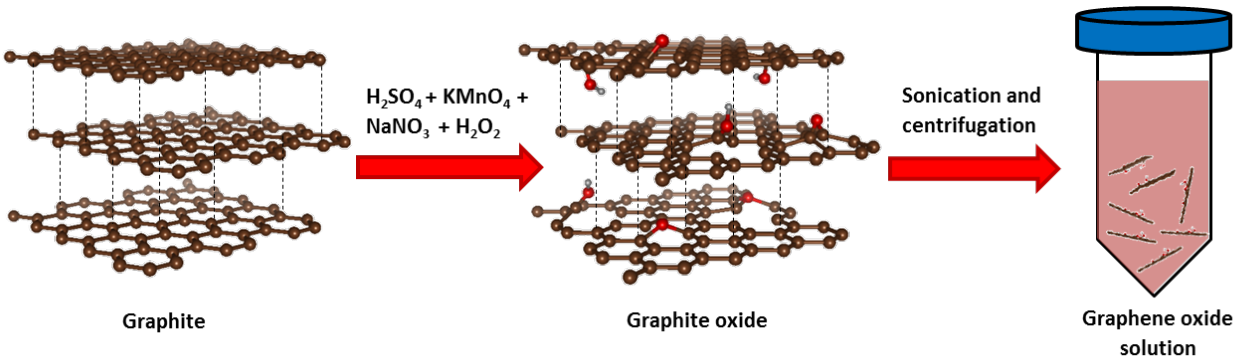

Fig. 1. Schematic representation of graphene oxide synthesis

2.2. GO membrane preparation

Graphene oxide suspension prepared as above can be easily transformed in the form of membranes using by either spraying the dispersion onto a porous template or by vacuum filtration of GO dispersion in the porous template. In the present work, we adopted the vacuum

filtration method to make thin membranes of graphene oxide on the PVDF templates with a pore size of 0.22 µm. Vacuum filtration of the GO dispersion produced a uniform film of graphene oxide on the template. Using this method, membranes with required thickness were produced by changing the volume of GO dispersion.

2.3. GO membrane characterization

Physical characterization of membranes prepared using above method was carried out extensively to ensure the characteristics before using as a membrane for filtration. For that purpose, initially scanning electron microscope (SEM) was used to confirm the surface morphology and laminated structure of graphene oxide membranes. X-Ray Diffraction (XRD) was used to assess changes in the crystallographic structure as well as to determine the interlayer spacing between laminates in the membrane**.**

The physical integrity of the flat membranes prepared was determined with a leak test[25]. It is essentially a container with an aperture covered by a GO membrane and filled with a desired solvent such as ethanol or water, which is kept on a computerized weighing scale. The custom-made setup and membrane performance are described in detail in section 3. For ensuring the membrane effectiveness, prior to the NOMs rejection test, other relatively larger (in hydrated radius > 0.45 nm) species such as $[Fe(CN)_6]^{3-}$, glycerol, and sucrose were tested on GO membranes via U-tube type experiments. Membranes after testing for species were taken out, rinsed in water, dried and again tested for ethanol vapor leak test (described in Fig. 3). For all these U-tube permeation experiments the permeate samples have been taken in regular intervals from 3 hrs to 120 hrs.

2.4. NOMs rejection test and water flux measurements

Samples of filtered water from the Sydney Water's Nepean Water Filtration Plant were used throughout this study. The filtered water was the product of the standard water treatment process at the plant, namely coagulation with $FeCl_3$ and a cationic polyDADMAC followed by filtration in deep bed filters. The dissolved organic carbon of the filtered water was 5 mg/L and the turbidity < 0.2 NTU.

We have used two methods (shown in Fig. 2) to insure error free NOMs removal and water flux measurements. In the first experiment, the NOMs containing water was fed on one side, and pure de-ionized water was on the permeate side of the U-tube (Fig. 2a). Chemical analyses such as ion chromatography (IC), inductively coupled plasma optical emission spectrometry (ICP-OES), dissolved organic carbon (DOC) of samples of both sides (of the u-tube shown in Fig. 2) were carried out for quantitative analysis of permeate. More specifically, a highly sensitive liquid chromatography-organic carbon detection (LC-OCD) test was extensively conducted to analyze the presence of NOMs in the feed and permeate solutions taken from the U-tube at regular intervals during the filtration experiment.

In the second experiment, a pressure controlled filtration method was used to accurately determine the water flux. The applied pressure P during filtration was controlled at $0.5 \leq P \leq 0.75$ bar while storing the permeate in a container kept on the weight scale. GO membranes of an average effective area of ~3.0 cm^2 were used for the filtration experiments.

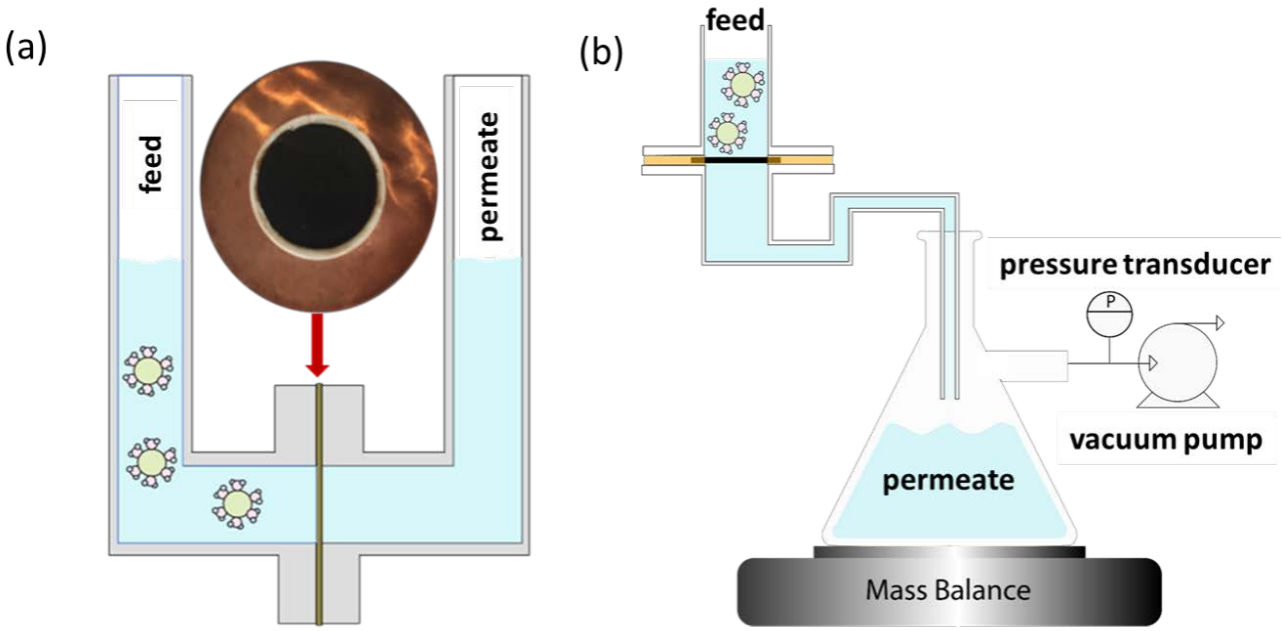

Fig. 2. Schematic of filtration set-up: a) U-tube setup for quantitative analysis with a digital photograph of the membrane assembly, b) Pressure controlled water flux measurement.

3. Results and Discussion

3.1. Membrane characterization results

In this section, properties of the membranes (with thickness values of 1, 2, 4, 6, 8 μm) produced by vacuum filtration method are discussed. SEM images in Fig. 3 show the surface morphology and cross-section of GO membrane/laminates. Fig. 3a shows the surface morphology of the membrane with wrinkle like regions indicating the folding of GO laminate whereas Fig. 3b illustrates the layer-by-layer laminated structure of our GO membrane. The spacing between two layers in the GO laminated structure was determined using X-Ray diffraction (Fig. 3c). The sharp peak at a 2θ value of 10.7° is equal to the d-spacing value of 8.25 Å for the membranes which is typical for GO membranes.

3.2. Membrane integrity analysis

To conduct the water flux and NOMs removal measurements with high accuracy, the GO membranes were tested for any possible physical leak or cracks. Initially, optical and scanning electron microscope were employed to observe if any physical cracks or micrometer-sized pores (unlike typical GO membrane) are present. We conducted a proof of concept experiment[25] to analyze the membrane for leaks via physical cracks of defects however the continuity of the membranes has also been seen using SEM (surface morphology) and optical microscope.

We know that a GO membrane should not allow permeation of any solvent vapors other than water. In our leaks test experiment (Fig. 3d and 3d') initially we filled the container with pure ethanol and continuously monitored the weight loss. The leak test shows no weight change with time which suggests ethanol molecules are not permeating through membranes. When we replaced ethanol of the container by water we observed a linear time-dependent weight loss which indicates the permeation of water vapors. Results of this test are shown in Fig. 3e. This test suggests that our membranes block ethanol molecules while water molecules diffuse through the GO membrane without any barrier which is in accordance with the theory proposed by Nair *et al*[25]. The leak test result demonstrates that the GO membranes are defect-free and have pores in sub-nanometer level or of the size of just above the water molecule's size.

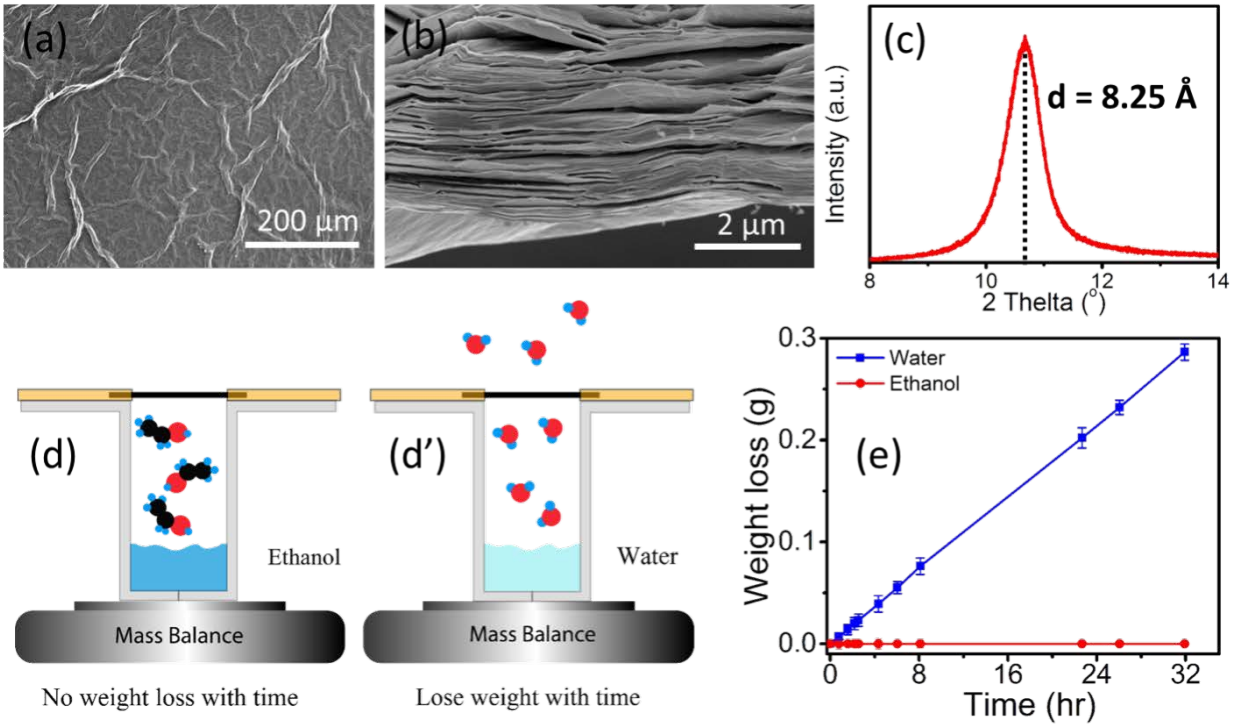

Fig. 3. Membrane Characterization: a) Surface morphology of a typical GO membrane, b) Cross-sectional image showing the laminated structure, c) X-ray diffraction pattern of GO membrane, d-d') Schematic of the experimental set-up for leak test, e) Graphical representation of weight loss with time for ethanol and water at 25 °C.

3.3. NOMs rejection test and Water flux

Prior to utilization for NOMs removal the membranes were tested for various other relatively larger (in hydrated radius > 0.45 nm) species such as $[Fe(CN)_6]^{3-}$, glycerol and sucrose. We observed that our membranes completely block the large ions of $[Fe(CN)_6]^{3-}$ and molecules of glycerol and sucrose. The observed ~100 % rejection of species of sizes above ~0.45 nm is expected for membranes of thicknesses between 1 and 8 µm. Membranes after testing for species were taken out, rinsed in water, dried and again tested for ethanol vapor leak test (described in Fig. 3). Our IC and ICP study shows nearly all the tested inorganic ions (Na^+, K^+, Cl^-, Mg^{2+}, Cu^{2+}, SO_4^{2-}) pass through the membrane with a nearly same rate which is consistent with previous studies[17]. These membranes however completely block (based on the total organic carbon analysis of the permeate) glycerol from passing the membranes. Similarly, we got no indication of the presence of $[Fe(CN)_6]^{3-}$ no matter how long we keep the experiment running for

filtration test in U-tube. For all these U-tube permeation experiments the permeate samples have been taken in regular intervals from 3 hrs to 120 hrs. Therefore, no signature of the tested species in absorption spectroscopy suggests that the permeate contains no solute species or below the detection limit (0.05 mg/L).

Once confirmed from the U-tube experiment that NOMs are completely rejected using GO membranes, we analyzed the water flux measurements experiments at a constant pressure of ~1.0 bar from the permeate side as shown in Fig. 2b. The detection limit of our LC-OCD technique is 5 ppb. Clearly, even the highly sensitive LC-OCD technique could not find any traces of NOMs in the permeate of the dead-end filtration process. Amount of water passing through the membrane was continuously measured with time. We made sure that the amount of water in the permeate should match with the amount reduced in the feed. Each experiment was repeated more than three times. Water flux values are shown in Fig. 4 are the average water flux for an experiment with deviation. Water flux was estimated using the equation:

$$J_w = \frac{Q}{AP\Delta t}$$

Where J_W is water flux; Q is water volume; A is the GO membrane size; P is vacuum pressure; and Δt gives the time.

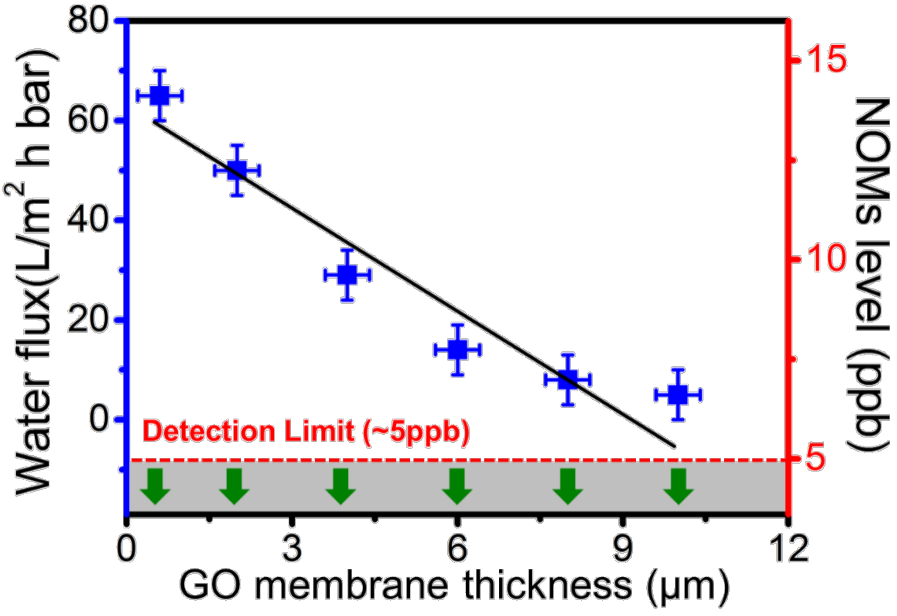

Fig. 4. Water flux and NOMs level in permeate side for GO membrane different thickness (Green arrows indicate NOMs level below the detection limit for each filtration experiment).

As expected thicker membranes have lower water flux. Thicker graphene oxide laminates have greater tortuosity and larger path for transport. The tortuosity is demonstrated in Fig. 5. The laminated structure of graphene oxide membrane is as a stack of a number of planes. If assumed that the transport of water molecules inside each graphene oxide laminate is Plane Poiseuille flow, the Hagen-Poiseuille equation can be applied here as:

$$Q \approx \frac{Gh^3}{12\mu} \quad G = (\frac{\Delta P}{dx})$$

Where Q is the volumetric flow rate per unit length, G is the pressure constant which can be given by $\frac{\Delta P}{dx}$ (ΔP is the pressure difference along the plane and dx is the transport length), h is space of the graphene oxide laminate and μ is the bulk water viscosity.

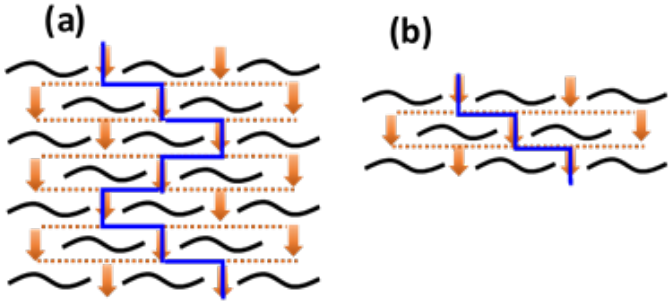

Fig. 5. Tortuosity of molecular transport in thick a) and thin b) GO membrane.

As h and μ are constant, Q is only determined by the pressure constant. It is found that the pressure difference will keep decreasing when the water molecules move layer by layer in graphene oxide membrane. Thus, the longer the tortuosity, the slower the volumetric flow rate. Fig. 5a and 5b show the relationship between the tortuosity and mass transport in GO-based membranes. The thicker GO laminates have greater tortuosity and larger path for transport than the thin GO laminates. Therefore, the highest water flow rate can only be achieved in thin GO membranes.

A highest water flux of ~65 *L m^{-2} h^{-1} bar^{-1}* has been achieved for a membrane with thickness < 1 μm using NOMs water in feed side. However, the similar thickness membrane shows a water flux of ~95 *L m^{-2} h^{-1} bar^{-1}* when we used the pure de-ionized water (no solute) at the feed side and 3.5 *L m^{-2} h^{-1} bar^{-1}* when the feed side has concentrated (1.0 M) sucrose solution. This is an interesting observation which contributes to understanding the mechanism. When we have concentrated feed solution (sucrose- 1.0 M), the impermeable solute species (sucrose) can be accumulated near membranes in the feed side during filtration which results into an impeded water transport via sub-nanometer capillaries and low water flux (3.5 *L m^{-2} h^{-1} bar^{-1}*). This effect will be weakened

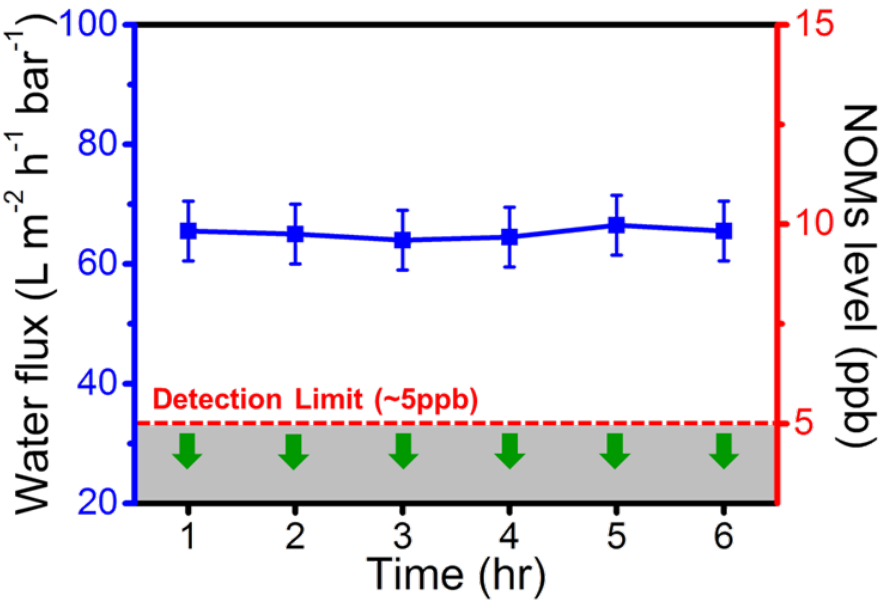

Fig. 6. Water flux at and NOMs level in permeate of GO (< 1 µm thick) membrane during the first 6 hours. Feed water has 5 mg/L- dissolved organic carbon (Green arrows indicate NOMs level below the detection limit for each filtration experiment).

For dilute feed solution, which is depicted by experimentally measured water flux of 95 *L* m^{-2} h^{-1} bar^{-1} for pure water (no solute) and 65 *L* m^{-2} h^{-1} bar^{-1} for NOMS water (5 mg/L DOC). The fast entrance of water molecule into laminates is mainly due to the sub-nanometer size capillary suction, and once the water molecules have entered the sub-nano channel, the pressure applied in line (from permeate side) with capillary suction contributes in the fast exit of water. To check the stability of water flux over time, we used a membrane with thickness (< 1 µm) for filtration test with 5 mg/L DOC on the feed side. The results shown in Fig. 6 (water flux vs. time) clearly indicates the suitability of GO membrane for water purification where constant flux over a longer period is required.

4. Conclusion

A novel membrane design was used to reject the natural organic matter with from drinking water. Constant high-water flux was achieved via the sub-nanometer capillary suction during filtration. The laboratory scale testing demonstrated that it is possible to reject >99.9 % (or below the detection limit of 5 ppb in the permeate) DOC from the water. A constant water flux of 65 *L* m^{-2} h^{-1} bar^{-1} for ~6.0 hours indicates that no short-term membrane fouling occurred. More research

is however needed to establish the longer-term fouling propensity of GO membranes. Our findings indicate that graphene-based membranes could be converted into alternative options to manage NOMs in conventional water treatment plants.

Acknowledgement

The authors thank Sydney Water for financial support and for permission to publish this work. Authors also thank Junjiao Deng and Technical Staff of the Analytical Centre of UNSW for their help.

References

[1] A. Matilainen, M. Vepsäläinen, M. Sillanpää, Natural organic matter removal by coagulation during drinking water treatment: A review, Adv. Colloid Interface Sci. 159 (2010) 189–197. doi:10.1016/j.cis.2010.06.007.

[2] D.T. Monteith, J.L. Stoddard, C.D. Evans, H.A. de Wit, M. Forsius, T. Høgåsen, A. Wilander, B.L. Skjelkvåle, D.S. Jeffries, J. Vuorenmaa, B. Keller, J. Kopácek, J. Vesely, Dissolved organic carbon trends resulting from changes in atmospheric deposition chemistry, Nature. 450 (2007) 537–540. doi:10.1038/nature06316.

[3] J.P. Ritson, N.J.D. Graham, M.R. Templeton, J.M. Clark, R. Gough, C. Freeman, The impact of climate change on the treatability of dissolved organic matter (DOM) in upland water supplies: A UK perspective, Sci. Total Environ. 473–474 (2014) 714–730. doi:10.1016/j.scitotenv.2013.12.095.

[4] R.L. Culp, Direct Filtration Author (s): Russell L . Culp Published by : American Water Works Association Stable URL : http://www.jstor.org/stable/41268992, 69 (2017) 375–378.

[5] H.C. Kim, M.J. Yu, Characterization of natural organic matter in conventional water treatment processes for selection of treatment processes focused on DBPs control, Water Res. 39 (2005) 4779–4789. doi:10.1016/j.watres.2005.09.021.

[6] M.A. Shannon, P.W. Bohn, M. Elimelech, J.G. Georgiadis, B.J. Mariñas, A.M. Mayes, Science and technology for water purification in the coming decades, Nature. 452 (2008) 301–310. doi:10.1038/nature06599.

[7] J. Lu, T. Zhang, J. Ma, Z. Chen, Evaluation of disinfection by-products formation during chlorination and chloramination of dissolved natural organic matter fractions isolated from a filtered river water, J. Hazard. Mater. 162 (2009) 140–145. doi:10.1016/j.jhazmat.2008.05.058.

[8] S.D. Richardson, M.J. Plewa, E.D. Wagner, R. Schoeny, D.M. DeMarini, Occurrence, genotoxicity, and carcinogenicity of regulated and emerging disinfection by-products in drinking water: A review and roadmap for research, Mutat. Res. - Rev. Mutat. Res. 636 (2007) 178–242. doi:10.1016/j.mrrev.2007.09.001.

[9] C. Wasko, A. Sharma, Steeper temporal distribution of rain intensity at higher temperatures within Australian storms, Nat. Geosci. 8 (2015) 527–529. doi:10.1038/ngeo2456.

[10] R.J. Norby, J.M. Warren, C.M. Iversen, B.E. Medlyn, R.E. McMurtrie, CO2 enhancement of forest productivity constrained by limited nitrogen availability, Proc. Natl. Acad. Sci. 107 (2010) 19368–19373. doi:10.1073/pnas.1006463107.

[11] M. Hu, B. Mi, Enabling graphene oxide nanosheets as water separation membranes, Environ. Sci. Technol. 47 (2013) 3715–3723.

[12] P.Z. Sun, M. Zhu, K.L. Wang, M.L. Zhong, J.Q. Wei, D.H. Wu, Z.P. Xu, H.W. Zhu, Selective Ion Penetration of Graphene Oxide Membranes, ACS Nano. 7 (2013) 428–437. doi:10.1021/nn304471w.

[13] Y. Han, Z. Xu, C. Gao, Ultrathin graphene nanofiltration membrane for water purification, Adv. Funct. Mater. 23 (2013) 3693–3700. doi:10.1002/adfm.201202601.

[14] F. Zhao, H. Cheng, Z. Zhang, L. Jiang, L. Qu, Direct Power Generation from a Graphene Oxide Film under Moisture, Adv. Mater. 27 (2015) 4351–4357. doi:10.1002/adma.201501867.

[15] I. Jung, D.A. Dikin, R.D. Piner, R.S. Ruoff, Tunable Electrical Conductivity of Individual Graphene Oxide Sheets Reduced at “Low” Temperatures, Nano Lett. 8 (2008) 4283–4287. doi:10.1021/nl8019938.

[16] F. Zhao, Y. Liang, C. Hu, L. Jiang, L. Qu, Highly efficient moisture-enabled electricity generation from graphene oxide frameworks, Energy Environ. Sci. 4 (2016) 1166–1169.

doi:10.1039/C5EE03701H.

[17] R.K. Joshi, P. Carbone, F.C. Wang, V.G. Kravets, Y. Su, I. V. Grigorieva, H.A. Wu, A.K. Geim, R.R. Nair, Precise and Ultrafast Molecular Sieving Through Graphene Oxide Membranes, Science (80-.). 343 (2014) 752–754. doi:10.1126/science.1245711.

[18] M. Mishra, R.K. Joshi, S. Ojha, D. Kanjilal, T. Mohanty, Role of oxygen in the work function modification at various stages of chemically synthesized graphene, J. Phys. Chem. C. 117 (2013) 19746–19750.

[19] O.C. Compton, S.T. Nguyen, Graphene oxide, highly reduced graphene oxide, and graphene: Versatile building blocks for carbon-based materials, Small. 6 (2010) 711–723. doi:10.1002/smll.200901934.

[20] W.S. Hummers, R.E. Offeman, Preparation of Graphitic Oxide, J. Am. Chem. Soc. 80 (1958) 1339–1339. doi:10.1021/ja01539a017.

[21] D.. C. Marcano, D.. V Kosynkin, J.M. Berlin, A. Sinitskii, Z.Z. Sun, A. Slesarev, L.B. Alemany, W. Lu, J.M. Tour, Improved Synthesis of Graphene Oxide, ACS Nano. 4 (2010) 4806–4814. doi:10.1021/nn1006368.

[22] C.-N. Yeh, K. Raidongia, J. Shao, Q.-H. Yang, J. Huang, On the origin of the stability of graphene oxide membranes in water, Nat. Chem. 7 (2015) 166–170. doi:10.1038/nchem.2145.

[23] B. Lian, J. Deng, G. Leslie, H. Bustamante, V. Sahajwalla, Y. Nishina, R.K. Joshi, Surfactant modified graphene oxide laminates for filtration, Carbon N. Y. 116 (2017) 240–245. doi:10.1016/j.carbon.2017.01.102.

[24] A.K. Geim, K.S. Novoselov, The rise of graphene, Nat. Mater. 6 (2007) 183–191. doi:10.1038/nmat1849.

[25] R.R. Nair, H.A. Wu, P.N. Jayaram, I. V. Grigorieva, A.K. Geim, Unimpeded Permeation of Water, Science (80-.). 335 (2012) 442–444. doi:10.1126/science.1211694.

[26] C.-N. Yeh, K. Raidongia, J. Shao, Q.-H. Yang, J. Huang, On the origin of the stability of graphene oxide membranes in water, Nat. Chem. 7 (2015) 166–170. doi:10.1038/nchem.2145.

[27] G. Zhao, X. Li, M. Huang, Z. Zhen, Y. Zhong, Q. Chen, X. Zhao, Y. He, R. Hu, T. Yang, R.

Zhang, C. Li, J. Kong, J.-B. Xu, R.S. Ruoff, H. Zhu, The physics and chemistry of graphene-on-surfaces, Chem. Soc. Rev. 46 (2017) 4417–4449. doi:10.1039/C7CS00256D.

[28] P. Sun, R. Ma, H. Deng, Z. Song, Z. Zhen, K. Wang, T. Sasaki, Z. Xu, H. Zhu, Intrinsic high water/ion selectivity of graphene oxide lamellar membranes in concentration gradient-driven diffusion, Chem. Sci. 7 (2016) 6988–6994. doi:10.1039/C6SC02865A.

[29] D.A. Dikin, S. Stankovich, E.J. Zimney, R.D. Piner, G.H.B. Dommett, G. Evmenenko, S.T. Nguyen, R.S. Ruoff, Preparation and characterization of graphene oxide paper, Nature. 448 (2007) 457–460. doi:10.1038/nature06016.

[30] J. Deng, Y. You, H. Bustamante, V. Sahajwalla, R.K. Joshi, Mechanism of water transport in graphene oxide laminates, Chem. Sci. 8 (2017) 1701–1704. doi:10.1039/C6SC03909J.

[31] B. Mi, Graphene Oxide Membranes for Ionic and Molecular Sieving, Science (80-.). 343 (2014) 740–742. doi:10.1126/science.1250247.

[32] H. Huang, Z. Song, N. Wei, L. Shi, Y. Mao, Y. Ying, L. Sun, Z. Xu, X. Peng, Ultrafast viscous water flow through nanostrand-channelled graphene oxide membranes, Nat. Commun. 4 (2013). doi:10.1038/ncomms3979.